Kibble-Zurek Mechanism in Topologically Nontrivial Zigzag Chains of Polariton Micropillars

D. D. Solnyshkov,[1] A. V. Nalitov,[1,2] and G. Malpuech[1]
[1]Institut Pascal, PHOTON-N2, Université Clermont Auvergne, CNRS, 4 Avenue Blaise Pascal, 63178 Aubière Cedex, France
[2]School of Physics and Astronomy, University of Southampton, Southampton SO17 1BJ, United Kingdom
(Received 15 June 2015; revised manuscript received 7 October 2015; published 29 January 2016)

We consider a zigzag chain of coupled micropillar cavities, taking into account the polarization of polariton states. We show that the TE-TM splitting of photonic cavity modes yields topologically protected polariton edge states. During the strongly nonadiabatic process of polariton condensation, the Kibble-Zurek mechanism leads to a random choice of polarization, equivalent to the dimerization of polymer chains. We show that dark-bright solitons appear as domain walls between polarization domains, analogous to the Su-Schrieffer-Heeger solitons in polymers. The soliton density scales as a power law with respect to the quenching parameter.

DOI: 10.1103/PhysRevLett.116.046402

As initially shown by Kibble [1] for the expansion and cooling of the early Universe, and then for liquid helium by Zurek [2], a system undergoing a second-order phase transition on a finite time scale develops domains with independent order parameters. The Kibble-Zurek mechanism (KZM) allows us to predict the typical size of the domains and, therefore, the densities of the topological defects on their boundaries. Their scaling as a function of the quench rate is given by a power law, with the critical exponent of the transition being determined by its universality class [3].

A very relevant system to study the KZM involves the quantum fluids such as atomic Bose-Einstein condensates (BECs) formed by cooling. Indeed, quantum fluids support topological defects [4,5], their most famous example being a quantum vortex, which, contrary to a classical vortex, like a tornado, cannot disappear "by itself" via a continuous transformation. This property is due to the difference in vortex and ground state topologies, which is guaranteed by the irrotational nature of the fluid described by a complex wave function [6]. The nonadiabatic cooling of such a fluid allows the development of topological defects obeying the KZM scaling, as confirmed by experiments [7] and also predicted for multicomponent BECs [8,9]. However, solitons in 1D and half vortices in 2D spinor BECs [4,5,10] are only quasitopological defects. Indeed, a dark soliton transforms into a grey one and eventually disappears by simple acceleration, and a half vortex can be unwound by a divergent magnetic field. Another system of interest for studying the KZM involves cavity exciton-polariton quantum fluids [11,12]. Because of the finite polariton lifetime, polariton condensation can be an out-of-equilibrium process driven by the condensation kinetics rather than by thermodynamics [12,13]. As previously pointed out [14,15], the establishment of a steady state by nonresonant pumping in an initially empty system cannot be an adiabatic process and is therefore equivalent to a quenching of the parameters of the system, leading to the appearance of topological defects.

Another class of systems which possess topologically protected states includes periodic lattices with topologically nontrivial band structures characterized by nonzero Chern numbers, or the Zak phase, depending on their dimensionality. The most well-known examples of such systems are the topological insulators [16], Kitaev chains supporting topologically protected Majorana states [17] and dimer chains [18]. Indeed, depending on the difference of the tunneling coefficients within and between the dimers, such chains form topologically different conduction bands, characterized by a π difference in the Zak phase [19]. As was shown recently [20], the number of states in the conduction band depends on this phase, and the states which are not included in the bulk are localized on the edges. These edge states do not rely on interparticle interactions but are topologically protected: they are robust against disorder and perturbations. Different implementations of topologically nontrivial band structures have been studied theoretically and experimentally in various systems, including photonics [21,22], optomechanics [23,24], excitons [25], and plasmonic zigzag chains [26–29]. Optical systems offer an important advantage compared to the electronic ones and to atomic BECs because of the facility of their fabrication and the complete accessibility of the wave function in time and real and reciprocal space. Polaritonic systems were shaped as molecules and lattices [30–32]. Schemes for creating polariton topological insulators have been proposed [33–36]. While KZM, as a universal mechanism, has already been widely studied in various systems sharing some common properties with our proposal, such as zigzag ionic chains [37–40], where the phase transition and the topology correspond to the physical arrangement of atoms, none of these possess

the same key ingredients. A topologically nontrivial polaritonic chain therefore appears as an ideal system for studying the complex interplay of topological ordering and KZM [41].

In this Letter, we describe a polariton BEC in a zigzag chain of polariton micropillars with photonic spin-orbit coupling (SOC) [34,42,43]. As a result, the polariton band is characterized by a nonzero Zak phase and the chain supports topologically protected edge states. These results are also valid for Rashba SOC present in atomic condensates [44]. We show that with a focused nonresonant excitation spot, condensation occurs on the edge states, with polarization determined by the Zak phase. When the system is excited homogeneously, a gas of dark-bright solitons [a spinor version of Su-Schrieffer-Heeger (SSH) solitons] is formed via the KZM. Here, the k^2 TE-TM SOC is crucial, allowing a homogeneous condensate, contrary to k-linear Rashba SOC. We demonstrate that the soliton density follows a power law with respect to the quenching parameter—pumping intensity. The scaling exponent for different system parameters is close to $1/4$, in agreement with the mean-field KZM theory for a 1D system.

Existence of topological edge states.—We first consider a zigzag chain of coupled 0D modes neglecting the spin, as is usually done in a theoretical analysis of the electronic dimer chains. Let us call the first pillar in the chain a, and let it be "below" the second pillar b so that the first link is oriented at 45° (see Fig. 1), which we will call the "diagonal" direction (D), while the perpendicular direction shall be "antidiagonal" (A, 135°). The pair ab forms the unit cell. Following the definitions established in previous works [20], the tunneling constant in the first link (within the cell) is called t', while the tunneling in the second link (between cells) is t. The corresponding tight-binding Hamiltonian reads (m is the cell number)

$$\hat{H} = \sum_m t' \hat{b}_m^\dagger \hat{a}_m + t \hat{a}_{m+1}^\dagger \hat{b}_m + \text{H.c.}, \tag{1}$$

where $\hat{a}$ and $\hat{b}$ operators act on the corresponding pillars.

Let us now consider that these 0D modes are constituted by photonic micropillars obtained by etching a planar cavity [45]. Each pillar ground state has two polarizations, which we assume to be degenerate. On the other hand, the optical eigenmodes of the cavity are TE and TM polarized and have different effective masses [46]. This makes the tunneling coefficients polarization dependent [34,42,43] and different for the polarizations oriented longitudinally and transversely with respect to the link. We therefore have $t < t'$ for D polarization, for which the first link (labeled by t') is longitudinal [see Figs. 1(a) and 1(d)], and $t > t'$ for the A polarization, for which the same link is transverse [see Figs. 1(b) and 1(e)]. The relative difference in the longitudinal and transverse tunneling coefficients for typical parameters of a polariton micropillar lattice can be on the order of 10% [34]. This difference of the tunneling coefficients is equivalent to the dimerization of polymer chains but associated with the polarization of the states. The corresponding dimers are shown with black dashed lines in Fig. 1.

For an even number of pillars, one can directly apply the SSH theory developed for polymer chains [18]. The dispersion of such a system contains two conduction bands, below and above the single-pillar energy, chosen as the zero reference. The existence of the edge state in this case is determined by the Zak phase, which is an analog of the Berry phase [47] defined on a unit cell of a size d for a Wannier function $u_{nk}(x)$, integrated over a given band n [19]:

$$\zeta_n = \int_{-\pi/d}^{\pi/d} \frac{2\pi}{d} \int_0^d u_{nk}^*(x) i \frac{\partial u_{nk}(x)}{\partial k} dx dk. \tag{2}$$

The Zak phase is determined by the ratio of the tunneling coefficients within and between the dimers [20]: $\zeta_n = 0$ if $t'/t > 1$, and $\zeta_n = \pi$ if $t'/t < 1$. The topological transition $\zeta_n = 0 \leftrightarrow \zeta_n = \pi$ occurs at $t = t'$. If the Zak phase is π, the number of states in the bulk is less than the number of pillars: $N = M - 2$, and the remaining states, whose energy is that of uncoupled modes, are localized on the edges of the chain. If the Zak phase $\zeta_n = 0$, the number of states in the bulk is equal to the number of pillars $N = M$, and no edge states appear. The advantage of the optical systems is that the Zak phase can be measured directly [27].

In our system, as can be deduced from Figs. 1(a) and 1(b), a pair of edge states does exist in one polarization (antidiagonal for our parameters), and does not exist in the other. The result of the diagonalization of the Hamiltonian

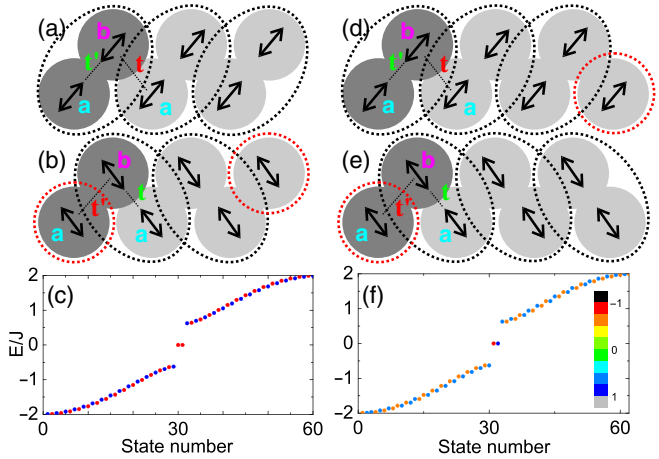

FIG. 1. A scheme of a zigzag chain with even and odd numbers of polariton pillars: a and b form a unit cell marked in dark grey. (a),(d) Diagonal polarization, $t' > t$. (b),(e) Antidiagonal polarization, $t' < t$. (c),(f) Energy band of 30 (c) and 31 (f) pillar chains obtained from the tight-binding Hamiltonian. The color shows the diagonal polarization degree of the states.

(1) with spin (see Ref. [48]) for a chain of 30 pillars ($\delta J = 0.3J$ for visibility) is shown in Fig. 1(c), with polarization shown in color. We see that the polarization states are interleaved, the lower band ends with polarization D, and the upper band begins with D, so the edge states (seen in the gap) are both necessarily A polarized. Rashba SOC gives a similar result. For an odd number of pillars, if $t/t' \neq 1$, one can redefine a dimer so that the Zak phase will be π and a state will appear on the edge which contains a unit cell broken by the boundary. For polaritons, an important consequence is that for one polarization (D), the edge state is on the right edge of the chain [see Fig. 1(d)], and for the other polarization (A) the edge state is on the left edge of the chain [see Fig. 1(e)]. Calculation yields Fig. 1(f), where for all states, including the edge ones, the polarization is interleaved.

Overall, whatever the number of pillars in a finite zigzag chain, because of the polariton SOC there are always two edge states in the system, either having the same polarization when the number of pillars is even or being cross polarized when the number of pillars is odd. The edge state polarization is always orthogonal to the axis linking the two last pillars at the chain edge.

We confirm the predictions of the analytical tight-binding model by solving numerically the spinor Schrödinger equation on a grid to find the eigenstates:

$$E\psi_{\pm} = -\frac{\hbar^2}{2m}\Delta\psi_{\pm} + \beta\left(\frac{\partial}{\partial x} \mp i\frac{\partial}{\partial y}\right)^2 \psi_{\mp} + U\psi_{\pm}, \quad (3)$$

where $\psi(\mathbf{r},t) = (\psi_+(\mathbf{r},t), \psi_-(\mathbf{r},t))^T$ are the two circular components of the wave function, $\beta = \hbar^2(m_l^{-1} - m_t^{-1})/4m$, while $m_{l,t}$ are the effective masses of TM and TE polarized particles, respectively, and $m = 2(m_t - m_l)/m_t m_l$; $m_t = 5 \times 10^{-5} m_0$, $m_l = 0.95 m_t$; m_0 is the free electron mass; and $U(\mathbf{r})$ is the potential of the pillars describing the confinement of polaritons in the chain beyond the tight-binding model [34]. The results of these calculations are presented in Fig. 2, showing the spatial images of the difference between the diagonal polarizations $I_D - I_A$ for both an even [Fig. 2(a)] and an odd [Fig. 2(b)] number of pillars. The localization length is discussed in the Supplemental Material [48].

Condensation on localized edge states.—A very effective way to excite these localized edge states is to create a polariton condensate using focused nonresonant pumping. This technique allows creation of strongly out-of-equilibrium states, typically the states showing the best spatial overlap with the localized excitonic reservoir induced by the pump [32,49,50]. In lattices, the repulsive potential induced by the excitonic reservoir becomes attractive for particles with a negative effective mass at the band edges, which leads to the condensation on localized gap states bound to the reservoir [32,50]. One expected peculiarity of the zigzag chain with a local pump

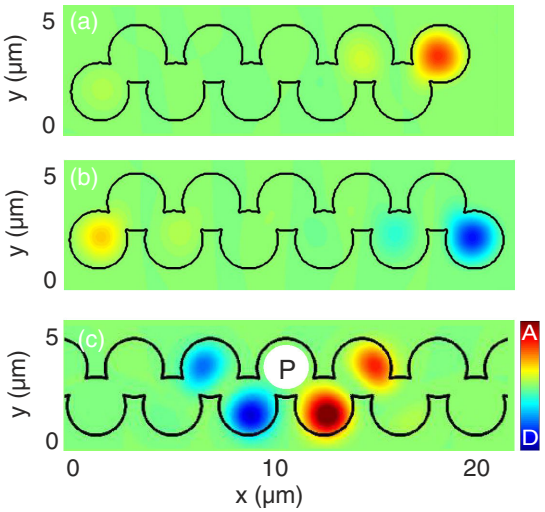

FIG. 2. Calculated spatial images of the difference in diagonal polarization emission $I_D - I_A$. (a) Edge states in a chain with an even number of pillars. (b) Edge states in a chain with an odd number of pillars. (c) Emission of the condensed states under localized pumping (marked P). Opposite diagonal polarization is observed on opposite sides.

is that the polarization of the localized mode where the condensation occurs is entirely fixed by the chain topology and the position of the pump, and it does not rely on a symmetry breaking process. To demonstrate this predicted feature, we model polariton condensation using the hybrid Boltzmann–Gross-Pitaevskii equation, which includes relaxation mechanisms [32,51,52]. For a thermal excitonic reservoir, the model can be reduced to

$$i\hbar\frac{\partial\psi_{\pm}}{\partial t} = -(1 - i\Lambda)\frac{\hbar^2}{2m}\Delta\psi_{\pm} + \beta\left(\frac{\partial}{\partial x} \mp i\frac{\partial}{\partial y}\right)^2 \psi_{\mp} + U\psi_{\pm} - \frac{i\hbar}{2\tau}\psi_{\pm} + \{[U_R + i\gamma(n)]\psi_{\pm} + \chi\}\exp\left(-\frac{(\mathbf{r} - \mathbf{r}_0)^2}{\sigma^2}\right), \quad (4)$$

where the parameters (values from Ref. [32]) other than in Eq. (3) are as follows: Λ, the kinetic energy relaxation term; U_R, the reservoir potential amplitude; σ, the reservoir width; τ, the lifetime; χ, the Gaussian noise term included to describe the spontaneous scattering [53,54]; $\gamma(n)$, the saturated stimulated scattering rate from the reservoir; and n, the total polariton density. We neglect the interactions within the condensate here. A pump located close to the edge will excite the unique localized mode at the edge of the chain. If the pumping spot is located in the bulk, the potential of the reservoir cuts the lattice into two smaller chains, and the same reasoning as above applies to each of them, leading to the condensation at their respective edge states. The results of the simulations for the pumping spot located in the middle of a chain (which allows us to check all predictions simultaneously) are presented in

Fig. 2(c), showing the difference between the intensities of the diagonal polarizations $I_D - I_A$ of the light emitted from the system above the condensation threshold. The condensation indeed occurs on the localized edge states on both sides of the spot, with polarization controlled by the condition on the Zak phase $\zeta_n = \pi$.

Spontaneous formation of dark-bright solitons via the Kibble-Zurek mechanism.—The consequences of the nontrivial topology of the system are truly revealed under *homogeneous* nonresonant pumping. While the previous results could be verified by purely linear measurements [27], in this section we study the condensation of polaritons, accompanied by the emergence of a spinor order parameter. As any second-order phase transition occurring on a finite time scale, it is described in terms of parameter quenching, responsible for the KZM-type formation of topological defects [1,2,7]. In a spinor system, the large phase fluctuations at the early stage of a condensation process are associated with spatial fluctuations of the polarization, governed by the phase difference between the spin components. The polarization domains correspond to the dimerization domains in the SSH picture, and the domain wall between them is equivalent to the SSH soliton [18]. These dark-bright solitons separate two polarization domains, both equally stable and characterized by a fixed difference π in their Zak phase. The stability of a dark-bright soliton, which cannot be destroyed by acceleration, is its most important feature: once formed, it does not disappear, contrary to a scalar dark or grey soliton. This stability requires the interactions in the condensate to be smaller than the TE-TM splitting [48]. It allows us to detect such objects in cw experiments, being advantageous with respect to the previous proposals of the KZM studies with polaritons [14,15], requiring single-pulse experiments.

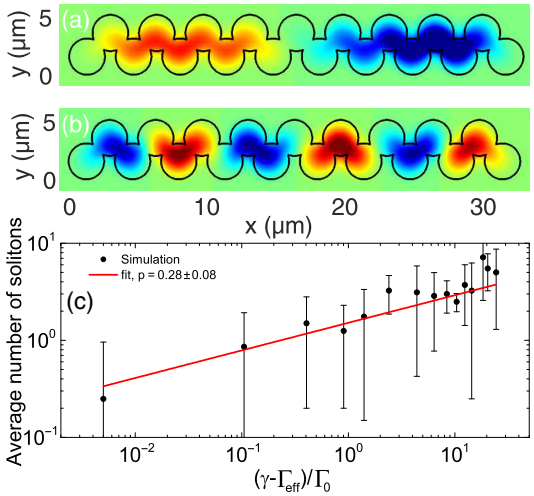

FIG. 3. (a),(b) Difference in diagonal polarization intensities for two examples of polarization textures in a zigzag chain. Colors are as in Fig. 2. (c) Average number of solitons as a function of effective pumping fitted by a power law.

Figure 3 shows the results of simulations based on the numerical solution of Eq. (4) with a homogeneous reservoir potential ($\sigma = \infty$) and interactions [48]. Figures 3(a) and 3(b) show the difference between the intensities of the diagonal polarizations $I_D - I_A$ of the light emitted by a condensate formed under weak and strong pumping, respectively. In Fig. 3(a), two domains A and D polarized corresponding to a single dark-bright soliton are visible. Figure 3(b) shows six polarization domains and five domain walls (for a movie, see the Supplemental Material [48]). In our numerical experiment, we do not change the temperature of the system, as in the classical KZM, but rather turn on the pumping and fill the system with particles, changing the critical condensation temperature, but keeping the system temperature (controlled by χ and Λ) constant. The quenching time is controlled by the pumping intensity $\tau_Q^{-1} \propto P$. This scheme, while being simpler and ubiquitously present in all polariton experiments, fits the KZM scheme because the relative temperature $\epsilon = (T - T_c)/T_c$ at threshold changes linearly with time (see the Supplemental Material [48]).

Indeed, the Gaussian noise χ is uncorrelated in time and thus creates a frequency-independent population of particles. However, the energy relaxation term proportional to Λ describes energy-dependent decay acting on these particles. The resulting spectral density $|\psi(E)|^2$ for the polariton state of energy E can be obtained as $|\psi(E)|^2 \propto \chi/\Gamma$, where Γ is the total decay rate, composed of energy-independent Γ_0 (ground state lifetime) and energy-dependent relaxation $\Gamma_\Lambda = \Lambda E$ [51], giving

$$|\psi(E)|^2 \propto \frac{\chi}{\Gamma_0 + \Lambda E} \approx \frac{\chi}{\Gamma_0}\left(1 - \frac{\Lambda E}{\Gamma_0}\right). \tag{5}$$

The linear part of the spectrum at low energies can be interpreted as a Boltzmann distribution function with an effective temperature $T = \Gamma_0/\Lambda$. Varying the relaxation efficiency, we can change this effective temperature: the better the relaxation, the lower the temperature. According to KZM, the average density of the topological defects n_{sol} in a BEC scales as the inverse healing length $\xi^{-1} = \xi_0^{-1}|\epsilon|^\nu$, where ν is a scaling exponent. In the mean-field approximation, $\nu = 1/2$ (because $\xi = \hbar/\sqrt{2\alpha n m}$, where α is the interaction constant), and the dynamical exponent is $z = 2$ [3,8] for relaxation linear in energy, which allows us to write $n_{\mathrm{sol}} = \xi_0^{-1}(\tau_0/\tau_Q)^{\nu/(1+z\nu)} \propto (\tau_0/\tau_Q)^{1/4}$. Thus, $n_{\mathrm{sol}} \propto \tau_Q^{-1/4} \propto \gamma^{1/4}$: a scaling exponent of $1/4$ is expected for the mean-field universality class. Figure 3(c) shows the number of solitons appearing in a chain of 40 pillars versus the effective pumping intensity $(\gamma - \Gamma_{\mathrm{eff}})/\Gamma_0$, where $\Gamma_{\mathrm{eff}} \approx 5.5\Gamma_0$ is the effective decay rate accounting for Λ. Each point is obtained as an average of ten simulations. The power law fit is compatible with the scaling exponent $1/4$ expected for KZM.

To conclude, we have demonstrated that the Zak phase plays a crucial role for the description of condensation in 1D zigzag chains of polariton pillars. Because of the SOC, such chains always exhibit exponentially localized edge states. Similar results can be obtained for Rashba or Dresselhaus SOC in atomic BECs. Under homogeneous pumping, dark-bright solitons appear between the domains of orthogonal polarization via the Kibble-Zurek mechanism. We extract numerically the dependence of the soliton density against the quenching parameters and find it in agreement with the analytical predictions. These domain walls can also be created by quasiresonant excitation, for example, using Gauss-Laguerre beams focused on a pillar chain (above the bistability threshold) [55]. They can also be manipulated using the electrically controlled in-plane effective magnetic fields [56], which might allow us to design optical racetrack memories [57].

We acknowledge our discussions with M. Glazov, A. Amo, and J. Bloch and the support of EU ITN INDEX (289968) and ANR Labex GANEX (207681).

[1] T. Kibble, J. Phys. A **9**, 1387 (1976).
[2] W. Zurek, Nature (London) **317**, 505 (1985).
[3] W. Zurek, Phys. Rep. **276**, 177 (1996).
[4] A. Leggett, *Quantum Liquids*, Oxford Graduate Texts (Oxford University Press, New York, 2006).
[5] G. Volovik, *The Universe in a Helium Droplet* (Clarendon Press, Oxford, 2003).
[6] L. Pitaevskii and S. Stringari, *Bose-Einstein Condensation*, International Series of Monographs on Physics Vol. 116 (Oxford University Press, New York, 2003).
[7] G. Lamporesi, S. Donadello, S. Serafini, F. Dalfovo, and G. Ferrari, Nat. Phys. **9**, 656 (2013).
[8] B. Damski and W. H. Zurek, Phys. Rev. Lett. **104**, 160404 (2010).
[9] J. Sabbatini, W. H. Zurek, and M. J. Davis, Phys. Rev. Lett. **107**, 230402 (2011).
[10] Y. G. Rubo, Phys. Rev. Lett. **99**, 106401 (2007).
[11] A. V. Kavokin, J. J. Baumberg, G. Malpuech, and F. P. Laussy, *Microcavities*, Series on Semiconductor Science and Technology Vol. 16 (Oxford University Press, New York, 2011).
[12] I. Carusotto and C. Ciuti, Rev. Mod. Phys. **85**, 299 (2013).
[13] J. Kasprzak, D. D. Solnyshkov, R. André, L. S. Dang, and G. Malpuech, Phys. Rev. Lett. **101**, 146404 (2008).
[14] M. Matuszewski and E. Witkowska, Phys. Rev. B **89**, 155318 (2014).
[15] T. C. H. Liew, O. A. Egorov, M. Matuszewski, O. Kyriienko, X. Ma, and E. A. Ostrovskaya, Phys. Rev. B **91**, 085413 (2015).
[16] M. Z. Hasan and C. L. Kane, Rev. Mod. Phys. **82**, 3045 (2010).
[17] A. Kitaev, Phys. Usp. **44**, 131 (2001).
[18] W. P. Su, J. R. Schrieffer, and A. J. Heeger, Phys. Rev. B **22**, 2099 (1980).
[19] J. Zak, Phys. Rev. Lett. **62**, 2747 (1989).
[20] P. Delplace, D. Ullmo, and G. Montambaux, Phys. Rev. B **84**, 195452 (2011).
[21] H. Schomerus, Opt. Lett. **38**, 1912 (2013).
[22] L. Lu, J. Joannopoulos, and M. Soljacic, Nat. Photonics **8**, 821 (2014).
[23] M. Schmidt, V. Peano, and F. Marquardt, New J. Phys. **17**, 023025 (2015).
[24] V. Peano, C. Brendel, M. Schmidt, and F. Marquardt, Phys. Rev. X **5**, 031011 (2015).
[25] J. Yuen-Zhou, S. K. Saikin, N. Y. Yao, and A. Aspuru-Guzik, Nat. Mater. **13**, 1026 (2014).
[26] A. Poddubny, A. Miroshnichenko, A. Slobozhanyuk, and Y. Kivshar, ACS Photonics **1**, 101 (2014).
[27] A. V. Poshakinskiy, A. N. Poddubny, and M. Hafezi, Phys. Rev. A **91**, 043830 (2015).
[28] A. P. Slobozhanyuk, A. N. Poddubny, A. E. Miroshnichenko, P. A. Belov, and Y. S. Kivshar, Phys. Rev. Lett. **114**, 123901 (2015).
[29] I. S. Sinev, I. S. Mukhin, A. P. Slobozhanyuk, A. N. Poddubny, A. E. Miroshnichenko, A. K. Samusev, and Y. S. Kivshar, Nanoscale **7**, 11904 (2015).
[30] N. Kim, K. Kusudo, A. Loeffler, S. Hoefling, A. Forchel, and Y. Yamamoto, New J. Phys. **15**, 035032 (2013).
[31] E. A. Cerda-Méndez, D. N. Krizhanovskii, M. Wouters, R. Bradley, K. Biermann, K. Guda, R. Hey, P. V. Santos, D. Sarkar, and M. S. Skolnick, Phys. Rev. Lett. **105**, 116402 (2010).
[32] T. Jacqmin, I. Carusotto, I. Sagnes, M. Abbarchi, D. D. Solnyshkov, G. Malpuech, E. Galopin, A. Lemaitre, J. Bloch, and A. Amo, Phys. Rev. Lett. **112**, 116402 (2014).
[33] T. Karzig, C.-E. Bardyn, N. H. Lindner, and G. Refael, Phys. Rev. X **5**, 031001 (2015).
[34] A. V. Nalitov, D. D Solnyshkov, and G. Malpuech, Phys. Rev. Lett. **114**, 116401 (2015).
[35] C.-E. Bardyn, T. Karzig, G. Refael, and T. C. H. Liew, Phys. Rev. B **91**, 161413 (2015).
[36] J. Yuen-Zhou, S. K. Saikin, T. H. Zhu, M. C. Onbasli, C. A. Ross, V. Bulovic, and M. A. Baldo, arXiv:1509.03687.
[37] A. del Campo, G. De Chiara, G. Morigi, M. B. Plenio, and A. Retzker, Phys. Rev. Lett. **105**, 075701 (2010).
[38] S. Ulm, J. Rossnagel, G. Jacob, C. Degunther, S. T. Dawkins, U. G. Poschinger, R. Nigmatullin, A. Retzker, M. B. Plenio, F. Schmidt-Kaler *et al.*, Nat. Commun. **4**, 2290 (2013).
[39] K. Pyka, J. Keller, H. L. Partner, R. Nigmatullin, T. Burgermeister, D. M. Meier, K. Kuhlmann, A. Retzker, M. B. Plenio, W. H. Zurek *et al.*, Nat. Commun. **4**, 2291 (2013).
[40] A. del Campo and W. H. Zurek, Int. J. Mod. Phys. A **29**, 1430018 (2014).
[41] A. Bermudez, D. Patanè, L. Amico, and M. A. Martin-Delgado, Phys. Rev. Lett. **102**, 135702 (2009).
[42] A. V. Nalitov, G. Malpuech, H. Tercas, and D. D. Solnyshkov, Phys. Rev. Lett. **114**, 026803 (2015).
[43] V. Sala, D. Solnyshkov, I. Carusotto, T. Jacqmin, A. Lemaitre, H. Tercas, A. Nalitov, M. Abbarchi, E. Galopin, I. Sagnes *et al.*, Phys. Rev. X **5**, 011034 (2015).
[44] Y.-J. Lin, K. Jimenez-Garcia, and I. B. Spielman, Nature (London) **471**, 83 (2011).

[45] L. Ferrier, E. Wertz, R. Johne, D. D. Solnyshkov, P. Senellart, I. Sagnes, A. Lemaítre, G. Malpuech, and J. Bloch, Phys. Rev. Lett. **106**, 126401 (2011).
[46] G. Panzarini, L. C. Andreani, A. Armitage, D. Baxter, M. S. Skolnick, V. N. Astratov, J. S. Roberts, A. V. Kavokin, M. R. Vladimirova, and M. A. Kaliteevski, Phys. Rev. B **59**, 5082 (1999).
[47] M. V. Berry, Proc. Phys. Soc. London Sect. A **392**, 45 (1984).
[48] See Supplemental Material at http://link.aps.org/supplemental/10.1103/PhysRevLett.116.046402 for extra results of numerical simulations.
[49] M. Galbiati, L. Ferrier, D. D. Solnyshkov, D. Tanese, E. Wertz, A. Amo, M. Abbarchi, P. Senellart, I. Sagnes, A. Lemaitre *et al.*, Phys. Rev. Lett. **108**, 126403 (2012).
[50] D. Tanese, H. Flayac, D. Solnyshkov, A. Amo, A. Lemaitre, E. Galopin, R. Braive, P. Senellart, I. Sagnes, G. Malpuech *et al.*, Nat. Commun. **4**, 1749 (2013).
[51] D. D. Solnyshkov, H. Terças, K. Dini, and G. Malpuech, Phys. Rev. A **89**, 033626 (2014).
[52] E. Wertz, A. Amo, D. D. Solnyshkov, L. Ferrier, T. C. H. Liew, D. Sanvitto, P. Senellart, I. Sagnes, A. Lemaître, A. V. Kavokin *et al.*, Phys. Rev. Lett. **109**, 216404 (2012).
[53] H. T. C. Stoff, J. Low Temp. Phys. **114**, 11 (1999).
[54] C. W. Gardiner, J. R. Anglin, and T. I. A. Fudge, J. Phys. B **35**, 1555 (2002).
[55] H. Flayac, D. Solnyshkov, and G. Malpuech, New J. Phys. **14**, 085018 (2012).
[56] D. D. Solnyshkov, H. Flayac, and G. Malpuech, Phys. Rev. B **85**, 073105 (2012).
[57] A. Fert, V. Cros, and J. Sampaio, Nat. Nanotechnol. **8**, 152 (2013).